ORIGINAL ARTICLE

Repurposing antimycotic ciclopirox olamine as a promising anti-ischemic stroke agent

Hongxuan Feng[a,d,†], Linghao Hu[b,c,†], Hongwen Zhu[a,†], Lingxue Tao[a,†], Lei Wu[a], Qinyuan Zhao[a,d], Yemi Gao[a], Qi Gong[a], Fei Mao[b], Xiaokang Li[b], Hu Zhou[a,*], Jian Li[b,c,*], Haiyan Zhang[a,d,*]

[a]CAS Key Laboratory of Receptor Research, Shanghai Institute of Materia Medica, Chinese Academy of Sciences, Shanghai 201203, China
[b]State Key Laboratory of Bioreactor Engineering, East China University of Science and Technology, Shanghai 200237, China
[c]Shanghai Key Laboratory of New Drug Design, School of Pharmacy, East China University of Science and Technology, Shanghai 200237, China
[d]University of Chinese Academy of Sciences, Beijing 100049, China

Abstract Ischemic stroke is a severe disorder resulting from acute cerebral thrombosis. Here we demonstrated that post-ischemic treatment with ciclopirox olamine (CPX), a potent antifungal clinical drug, alleviated brain infarction, neurological deficits and brain edema in a classic rat model of ischemic stroke. Single dose post-ischemic administration of CPX provided a long-lasting neuroprotective effect, which can be further enhanced by multiple doses administration of CPX. CPX also effectively reversed ischemia-induced neuronal loss, glial activation as well as blood−brain barrier (BBB) damage. Employing quantitative phosphoproteomic analysis, 130 phosphosites in 122 proteins were identified to be significantly regulated by CPX treatment in oxygen glucose deprivation (OGD)-exposed SH-SY5Y cells, which revealed that phosphokinases and cell cycle-related phosphoproteins were largely influenced. Subsequently, we demonstrated that CPX markedly enhanced the AKT (protein kinase B, PKB/AKT) and GSK3β (glycogen synthase kinase 3β) phosphorylation in OGD-exposed SH-SY5Y cells, and regulated the cell cycle progression and nitric oxide (NO) release in lipopolysaccharide (LPS)-induced BV-2 cells, which may contribute to its ameliorative effects against ischemia-associated neuronal death and microglial inflammation. Our study suggests that CPX could be a promising compound to reduce multiple ischemic injuries; however, further studies will be needed to clarify the molecular mechanisms involved.

*Corresponding authors. Tel./fax: +86 21 50806710.
E-mail addresses: zhouhu@simm.ac.cn (Hu Zhou), jianli@ecust.edu.cn (Jian Li), hzhang@simm.ac.cn (Haiyan Zhang).
†These authors made equal contributions to this work.

1. Introduction

Ischemic stroke, an acute disturbance of brain function, is a leading contributor to morbidity and mortality globally. Currently, ischemic stroke has remained essentially an unmet medical need. As a matter of fact, there have been limited advances for the clinical treatment of ischemic stroke, except the recombinant tissue plasminogen activator, which has been proven to be restricted to a small portion of ischemic stroke patients due to a narrow time window and the risk of hemorrhagic transformation.

Alternatively, neuroprotective research has gained significant progress and remains as a promising option for the treatment of stroke, although the road toward achieving satisfactory neuroprotection in stroke patients is still extremely challenging. First, the history of acute ischemic stroke has largely developed over the past 30 years, from a simple vascular disease to a neurovascular disease involving a triad consisting of neuron, microglia, astrocyte, pericyte and endothelial cells, and was lately expanded to be a vascular neural network disease even include the venous system, which further enhances our understanding of the underlying complicated mechanisms of ischemic stroke and the way to conquer it. Second, various drugs with promising multifaceted therapeutic targets have been demonstrated to show promising preclinical or clinical effects against stroke, such as DL-3-*n*-butylphthalide and statins[1–6]. Third, the success of endovascular thrombectomy provides new hope for ischemic stroke therapy and has created great opportunity for better estimating the effectiveness of neuroprotective agents[7,8]. Given such challenges and opportunities, it is of great importance and necessity to discover novel and potent neuroprotective agents against ischemic stroke.

Currently, translation of therapies that target post-ischemic deleterious mechanisms is still facing a difficult bottleneck, as massive evidences support the idea that ischemic stroke is a severe disease with multi-facet pathological changes, which includes impaired energy metabolism, altered ion homeostasis, free radical production, and aberrant immune response[9,10]. Due to lack of efficient therapeutic target, phenotypic screening is currently expected as one of the most popular strategies for discovery of drugs against the complexity of multifactorial diseases including ischemic stroke[11,12], which may also offer additional opportunity to identify novel multipotent neuroprotective agents[13,14]. Here, employing a well-accepted *in vitro* phenotypic cellular model for ischemic stroke[4,15], we screened 778 drugs approved by the United States Food and Drug administration (Supporting Information Fig. S1A) and luckily identified three drugs with significant protective effects against oxygen glucose deprivation (OGD)-stimulated cytotoxicity in SH-SY5Y cells (Supporting Information Table S1), including the target compound of the present study, ciclopirox olamine (CPX, Fig. S1B).

Accumulating evidence clearly indicates that CPX is a well-known antifungal clinical drug, which is lately demonstrated to possess potential therapeutic effects against other diseases, including cancer, diabetes, and HIV infection[16]. However, to our knowledge, no study was systematically conducted on assessing the effects of CPX on ischemic brain injury, except some evidences indicating its advantage effects on other cardiovascular diseases and neuroprotective effects *in vitro*[17–21]. Here in this study, the off-patent synthetic antimicrobial CPX is used for the very first time to influence the pathophysiology of brain ischemia in a middle cerebral artery occlusion (MCAO) rat model. CPX with multiple doses post-ischemic administration exhibited superior anti-ischemic efficacy, as compare to single dose post-ischemic administration of CPX and positive control, edaravone. CPX acted as potent regulator of protein phosphorylation, especially to kinases and cell cycle proteins in neuronal cells, and was also able to directly ameliorate ischemic insults-induced neuronal damage and glial inflammation.

2. Materials and methods

2.1. Drug administration

CPX (Sigma–Aldrich, St. Louis, MO, USA) was dissolved in dimethyl sulfoxide (DMSO) at 10 mmol/L as stock solution and diluted before drug administration. In the *in vivo* experiments, CPX powder was dissolved by saline and diluted to the concentrations for intravenous administration. CPX was administered intravenously immediately after withdrawing the monofilament. For the long-term effects of CPX evaluation, single dose of 3 mg/kg of CPX was administrated immediately after withdrawing the monofilament, while multiple doses were first administrated same as the single dose, then continuously administrated every 24 h for 7 days. For the OGD study, cells were incubated with indicated concentrations of CPX when exposed to OGD.

2.2. Cell culture, OGD insults and cell viability assay

Details are described in the Supporting Information.

2.3. Animals

Male SD (Sprague–Dawley) rats (7–8 weeks old) weighing 230–300 g were obtained from the Animal Center of Shanghai Institute of Materia Medica (Shanghai, China). All the experimental procedures approved by the animal Care and Use Committee of Shanghai Institute of Materia Medica (Shanghai, China). Efforts were made to minimize the pain of animals and reduce the number of experimental animals. Reporting of this work complies with ARRIVE (animal research: reporting of *in vivo* experiments) guidelines. Animals were housed under 12 h day/night cycle with freely accessible to food and water. A total of 471 rats were included in the study. Data were analyzed on 307 rats, and 164 rats were

excluded from the experiment due to death or failure of MCAO surgery. The animal numbers of individual experiments in the detail were listed in Supporting Information Table S2. The animals were randomly assigned into different groups before surgery.

2.4. Middle cerebral artery occlusion (MCAO)

The surgery was performed as previously described[22]. Briefly, rats were anesthetized with intraperitoneally administration of 400 mg/kg chloral hydrate (except the cohort study for the effect of CPX administrated 4.5 h after MCAO was anesthetized by isoflurane), then a surgical monofilament nylon suture (Sunbio Biotech Co. Ltd., Beijing, China) was inlet into the left internal carotid artery (ICA) through the external carotid artery (ECA) stump to block the origin of the middle cerebral artery (MCA). The suture was placed there for 2 h resulting in ischemic injury and then removed to induce reperfusion of the MCA. The rats of sham group underwent the same procedures except occlusion of the MCA. The animals were returned to cages after fully awaken.

2.5. Neurological function assessment

Neurological function was evaluated at 24 h after reperfusion according to the guidelines of the modified neurological severity scores (mNSS), which was used for assessment of neurological deficits including motor, visual, tactile and reflex responses and proprioception (scale: 0–18, no neurological deficits was scored as 0; maximal neurological deficits was scored as 18)[23]. The whole assessment was performed by an experimenter who was blind to the grouping.

2.6. Measurement of infarct volume

Infarct volume was measured immediately following neurological function assessment with the methods of TTC (triphenyltetrazolium chloride; Sinophar Chemical Reagent Co. Ltd., Shanghai, China) staining. Briefly, the experimental animals were fully anaesthetized and sacrificed. The brains were quickly frozen for 5 min, and sliced into six coronal sections, and then incubated with 1% TTC solution for 15 min at 37 °C water-bath away from light, then fixed with freshly prepared paraformaldehyde solution (4%) for 24 h. The images of brain sections were taken by digital camera and analyzed using ImagePro Plus software (Media Cybernetics, Silver Spring, MD, USA). The infarct volume was calculated as a percentage according to Eq. (1):

Infarct volume (%) = (Area of contralateral hemisphere–Area of non-infarcted region of ipsilateral hemisphere)/
Area of contralateral hemisphere × 100   (1)

2.7. Immunofluorescence

Rats were euthanized and perfused with 4% paraformaldehyde at 24 h after reperfusion. The brains were fixed in 4% paraformaldehyde overnight, then immersed in 20% and 30% sucrose for 3 days for dehydration, and then frozen in the Cryostat

Microtome (SM2000R, LEICA, Nussloch, Germany). The frozen brains were sliced into 30 μm-thick sections at the position of bregma approximating 0.5 to −0.5 mm using Cryostat Microtome (Leica, Buffalo Grove, IL, USA). The sectioned tissues were placed on slides. After blocking, the sections were incubated with indicated primary antibodies: anti-GFAP (glial fibrillary acidic protein) (1:100, Cell Signaling Technology, Beverly, MA, USA) or anti-IBA-1 (ionized calcium binding adaptor molecule-1) (1:200, Wako, Richmond, VA, USA) at 4 °C overnight. For the CD31 (platelet endothelial cell adhesion molecule-1, PECAM-1/CD31) and ZO-1 (zonula occludens 1) immunofluorescence, MCAO rats were sacrificed at 72 h after reperfusion and perfused with saline. After fixation with acetone, the brains were cryosliced, and the sections were treated with the primary antibodies: anti-CD31 (1:50, BD Biosciences, San Jose, CA, USA), or anti-ZO-1 (1:50, Invitrogen, Rockford, IL, USA) at 4 °C overnight. Sections were then treated with the secondary antibodies for 2 h at room temperature followed by 10 min incubation with DAPI (4′,6-diamidino-2-phenylindole dihydrochloride). After incubation and rinsing, the ipsilateral cerebral cortexes were visualized with Leica SP8 fluorescence microscope (LEICA, Nussloch, Germany).

2.8. TUNEL (terminal deoxynucleotidyl transferase dUTP nick end labeling) staining

Cell death was determined by using the In Situ Cell Death Detection Kit (Roche Diagnostics, Mannheim, Germany) according to protocol provided by the manufacturers. Briefly, brain sections were incubated with TUNEL reaction mixture away from light. Then, the sections were incubated with DAPI. After the last wash, images were taken by fluorescence microscopy. The number of TUNEL-positive cells and total cells were calculated in each field. Apoptotic rate was shown as the average percentage of TUNEL-positive cells to the total cells in the three fields selected for each section from ipsilateral cortex.

2.9. Evans blue assay

The disruption of blood−brain barrier (BBB) was evaluated by measuring the Evans blue content. MCAO or sham rats at 72 h after surgery were injected with 2% Evans blue (4 mL/kg, Sigma−Aldrich). The rats were euthanized 2 h after Evans blue injection and perfused with saline to fully remove the intravascular dye. Ipsilateral and contralateral hemispheres (without olfactory bulbs or cerebellum) were separated and their weights were recorded. Then the brains were homogenized in 1 mL 50% trichloroacetic acid and centrifuged ($10,000 \times g$, 20 min). The concentrations of Evans blue in the supernatants were measured at 620 nm absorbance and then determined with standard curves. The amounts of Evans blue were expressed as μg/g of wet tissue weight.

2.10. Rotarod test

The motor coordination of the rats was assessed with the accelerating rotarod (IITC Life Science, CA, USA) as described previously with minor modification[24]. All rats were habituated for 2

days before surgery. The sham or MCAO rats were placed on the accelerating rotarod, and the speed was increased linearly from 2 r.p.m to 20 r.p.m. within 120 s. The latency of the rats to fall from the rotating drum was recorded. Rotarod test was performed at 1, 3, 5, and 7 days post-surgery.

2.11. ELISA for TNF-α, IL-1β and IL-6

The cortexes of the 3 brain sections were collected and sonicated by ultrasound homogenization in ice-cold lysis buffer. The supernatants were collected by centrifugation ($14,000 \times g$, 15 min). The levels of tumor necrosis factor-α (TNF-α), interleukin-1β (IL-1β) and interleukin-6 (IL-6) were measured by the ELISA kits (R&D Biosystems, Minneapolis, MN, USA). The amounts of the inflammatory cytokines were normalized to the protein level of the supernatants.

2.12. Phosphoproteomic study

Details are described in the Supporting Information.

2.13. Bioinformatics analysis

The phosphoproteomic data analysis was mainly conducted using Excel and R software. The t-test P value and fold change between "OGD" and "OGD+CPX" of each site were calculated and the volcano plot was completed in Excel. Sites with a P value < 0.05 and a minimal fold change of >1.2 or <0.83 were determined to be significantly regulated. Kinases for substrate phosphosites were predicted by NetworKIN 3.0[25]. Only up-regulated phosphosites with a NetworKIN score >3 were reserved for dotplot representation. The gene ontology (GO) biological process enrichment analysis was performed using the STRING database and the result was plotted in R.

2.14. Western blot analysis

SH-SY5Y cells were lysed on ice for 30 min with radio-immunoprecipitation assay (RIPA) lysis buffer, then were centrifuged $12,000 \times g$ for 15 min. After the centrifugation, the supernatants were collected for further concentration assay and Western blot analysis. For the tissue sample preparation, cortex portions of the 3 brain slices were homogenized in the RIPA lysis buffer using an ultrasound sonicator, and then lysed on ice for 30 min. The supernatants were then collected by centrifugation ($12,000 \times g$, 15 min). To detect the level of occludin, the cortex of brain was collected at 72 h after reperfusion and processed as above described. The protein concentrations were determined by bicinchoninic acid Protein Assay Kit (Thermo Scientific, Rockford, IL, USA). Other details are described in the Supporting Information.

2.15. Lipopolysaccharide (LPS) stimulation and nitric oxide (NO) assay

The accumulated nitrite released into culture media was measured by Griess reagent (Sigma−Aldrich), which was an indication of microglial production of NO. Briefly, BV-2 cells were seeded into 96-wells and cultured for 24 h to fully attach on the plate. The cells were incubated with different concentrations of CPX for 2 h before stimulation with 100 ng/mL LPS (Sigma−Aldrich). After 24 h stimulation, the culture media was collected and centrifuged to discard the cell debris ($500 \times g$, 5 min). Then, cell cultured medium was fully mixed with Griess reagent (50 μL:50 μL) following by 15 min incubation at room temperature away from light. The 540 nm absorbance was measured on the Beckman DTX 800 Multimode Detector (Beckman, Coulter, Fullerton, CA, USA), and a series of concentrations of sodium nitrite was used as a standard for quantification.

2.16. Cell cycle analysis

The PI (propidium iodide, Sigma−Aldrich) staining was used to detect cell cycle. After 24 h stimulation with LPS, the cells were fixed with 70% ethanol at -20 °C overnight, following by incubation with RNase A (Sigma−Aldrich), and then stained with PI on ice for 15 min. Cell cycle distribution was then analyzed by flow cytometry (BD Biosciences, San Jose, CA, USA).

2.17. PathScan® intracellular signaling array analysis

The expressions of phosphorylated proteins by serine/threonine kinases after treatment with CPX were analyzed by the usage of PathScan® intracellular signaling array kit (Cell Signaling Technology). Briefly, after OGD injury and cultured under normal conditions for 15 min, SH-SY5Y cells were harvested and lysed with the cell lysis buffer on ice. The experiment was performed in strict accordance with the instructions of manufacturer and digital images were taken by the LI-COR Odyssey Imaging system (LI-COR, Lincoln, NE, USA). Then, the RFU intensity of each dot was analyzed by the Image studio software. Finally, a heat map of the average RFU intensity was drawn by the using "pheatmap" package in R software.

2.18. Statistical analysis

Data were presented as mean $\pm$ SD. Student's t-test was used to determine the statistical significance between two groups. One-way ANOVA (analysis of variance) followed by Turkey's tests were used to analyze the differences of multiple comparisons. The neurological scores were analyzed by Kruskal−Wallis nonparametric test followed by Dunn's multiple comparisons test. For Rotarod test data, two-way repeated measures ANOVA was performed, and then the difference between treatment groups at each time point were analyzed by Bonferroni-corrected *post hoc* comparisons. Statistical significance was established at $P < 0.05$.

3. Results

3.1. CPX treatment alleviated brain infarction, neurological deficits and brain edema induced by MCAO

As an extension of *in vitro* protective effects of CPX on SH-SY5Y cells suffering from OGD (Supporting Information Fig. S1), the *in vivo* effects of CPX against brain ischemic injury were examined in MCAO rats. Quantitative assessment of TTC-stained brain slices indicated that CPX treatment immediately after reperfusion reduced the infarction volume compared with vehicle group as shown by TTC staining (Fig. 1A and B). CPX (1, 3 and 10 mg/kg) significantly reduced the infarct volume by 13.12%, 22.45% and 11.92% (Fig. 1B). Administration of edaravone (10 mg/kg) also reduced the infarct area by 17.07%.
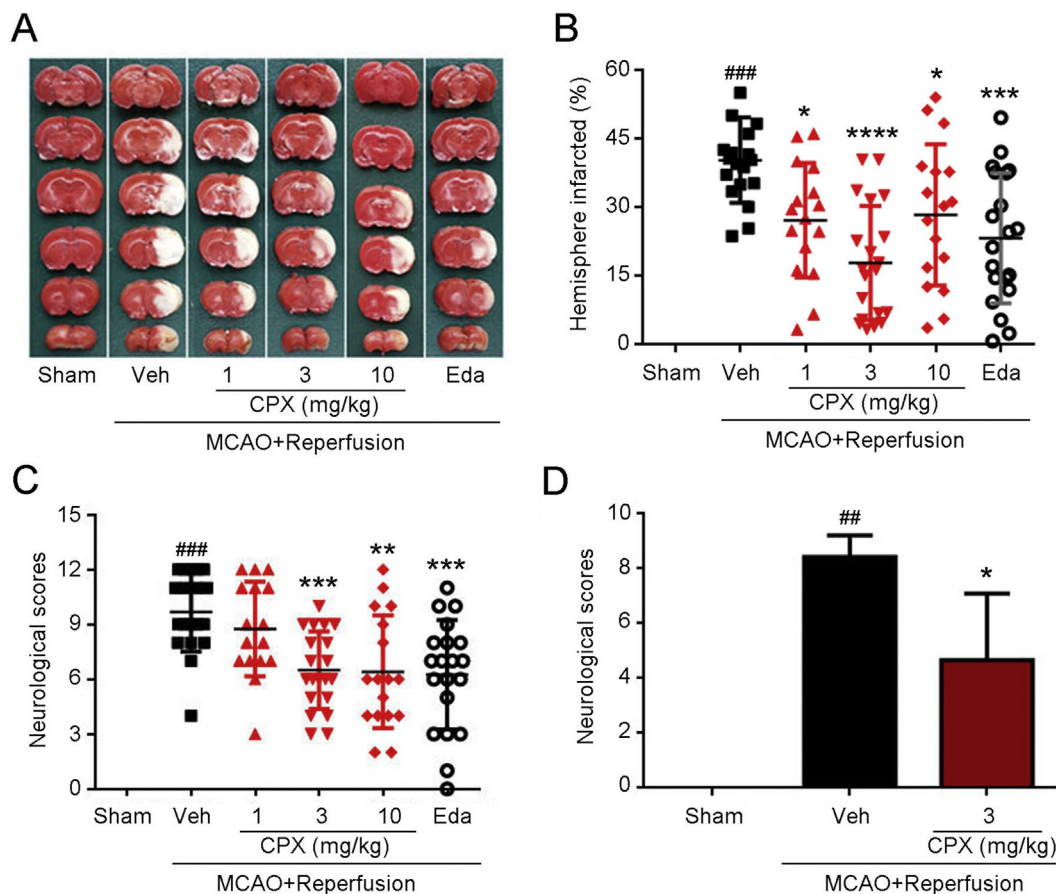
Figure 1 CPX reduced infarct volume and neurological deficits of MCAO rats. (A) Representative TTC staining. (B) Quantification of infarct volumes, $n = 16-20$ (except sham group $n = 5$). (C) Effects of CPX on the neurological deficits, $n = 16-20$ (except sham group $n = 5$). (D) Effect of CPX administration at 4.5 h after MCAO on neurological deficits tested 24 h after MCAO surgery (Sham, $n = 3$; Veh: MCAO rats treated with vehicle, $n = 7$; CPX: MCAO rats treated with 3 mg/kg CPX, $n = 6$; MCAO surgery was performed under isoflurane anesthetization). $^{\#\#}P < 0.01$, $^{\#\#\#}P < 0.001$ *versus* sham group; $^{*}P < 0.05$, $^{**}P < 0.01$, $^{***}P < 0.001$, $^{****}P < 0.0001$ *versus* vehicle-treated MCAO group. Veh: vehicle; Eda: edaravone.

Consistent with the decrease of infarct volume, neurological deficits of MCAO rats were also obviously alleviated by treatment with CPX at 3 and 10 mg/kg (Fig. 1C). Thus, 3 mg/kg of CPX has optimal efficacy against the brain ischemic injury, which was chosen as the appropriate dose for further study. Consistent with above results, CPX at 3 mg/kg dosage also alleviated brain edema shown as reduced brain water content (Supporting Information Fig. S2). Moreover, in order to evaluate the potential therapeutic time window of CPX for ischemic stroke treatment, we further assessed the effect of CPX against ischemic injury when administered at 4.5 h after MCAO surgery. To our delight, CPX administrated at 4.5 h after MCAO surgery (under isoflurane anesthetization) still markedly ameliorated MCAO-induced neurological deficits (Fig. 1D). We further analyzed the long-term efficacy of multiple doses of CPX administrated at 4.5 h, 1 and 3 days after MCAO surgery (under isoflurane anesthetization). As shown in Supporting Information Fig. S3A, CPX administration at 3 mg/kg significantly alleviated MCAO-induced neurological dysfunction [time: F $(3,31) = 5.962$, $P = 0.0025$, treatment: F $(3,31) = 9.544$, $P = 0.0042$, interaction: F $(3,31) = 1.887$, $P = 0.1523$]. In addition, CPX treatment also had a tendency to decrease the mortality rate of the rats suffering from MCAO (log-rank test,

$P = 0.1281$) (Fig. S4B). Above results demonstrated that 4.5 h post-ischemia administration of CPX still protected the animals against the ischemia/reperfusion-induced injuries.

3.2. Long-term effects of CPX on the motor dysfunction and brain infarction of MCAO rats

The motor functional recovery was further observed to assess the long-lasting anti-ischemic effect of CPX and compare the effects of single dose and multiple doses administration strategy in rats subjected to MCAO. Rotarod assay was performed, and the latency to fall off from the rod was recorded. Strategies of single dose administration of CPX immediately after reperfusion with or without multiple doses of continuous administration of CPX for 7 days were adopted to study the long-term effects of CPX on motor functional recovery (Fig. 2A). In the rotarod test, the latencies to fall off from the rotating rod on days 1, 3, 5, 7 after MCAO surgery were significantly decreased (Fig. 2B) [time: F $(4,96) = 80.53$, $P < 0.0001$, treatment: F $(1,24) = 231.2$, $P < 0.0001$, interaction: F $(4,96) = 63.32$, $P < 0.0001$]. The single dose and multiple doses administration of CPX both significantly alleviated motor dysfunction of the MCAO rats on days 1, 3, 5 and 7 after MCAO surgery (Fig. 2B) [single dose:
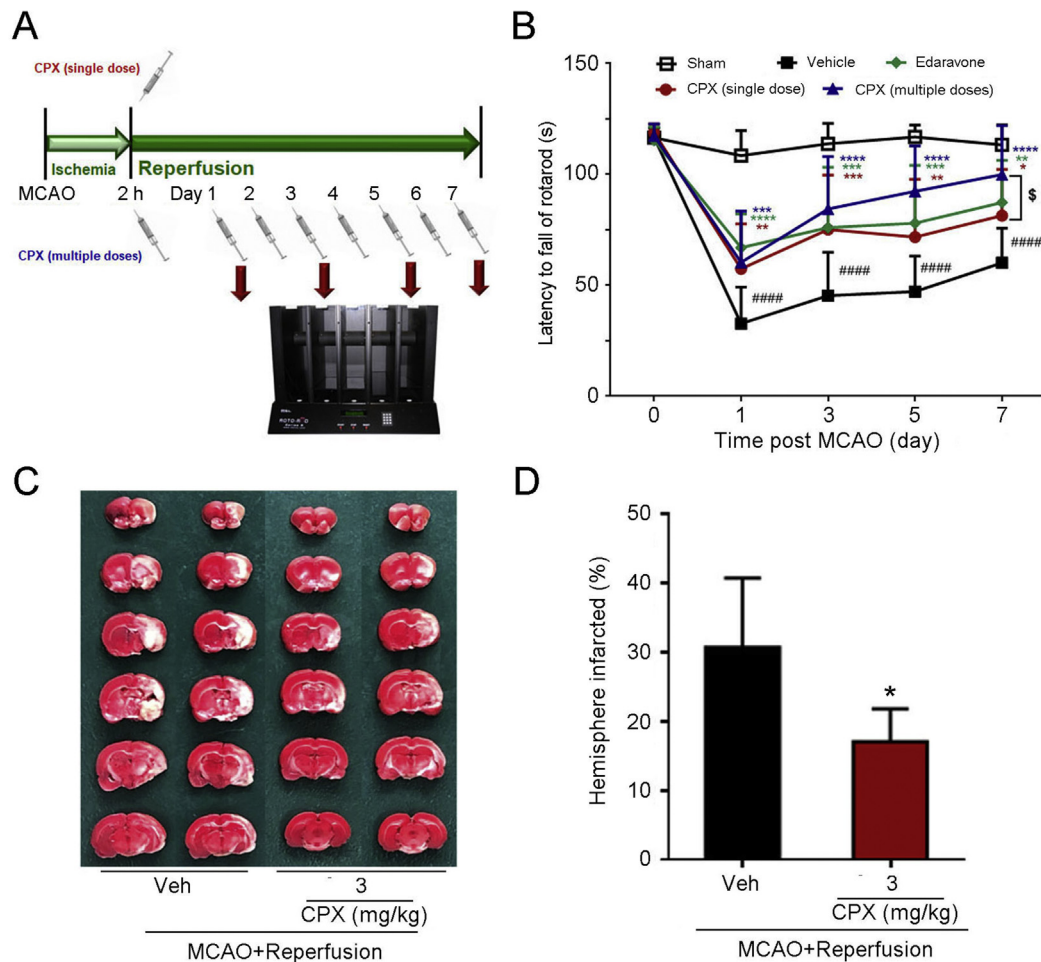
Figure 2 CPX treatment improved motor function of rats at 1, 3, 5 and 7 days after MCAO. (A) Experimental scheme of the single dose and multiple doses administration of CPX. (B) Effects of CPX treatment on the latency fall off the Rotarod of MCAO rats, $n = 9-15$. (C) Representative TTC staining of multiple doses administration of CPX at 7 days after MCAO. (D) Quantification of infarct volumes of multiple doses administration of CPX at 7 days after MCAO, $n = 5-6$. ####$P < 0.0001$ *versus* sham group; $^*P < 0.05$, $^{**}P < 0.01$, $^{***}P < 0.001$, $^{****}P < 0.0001$ *versus* vehicle-treated MCAO group; $^\$P < 0.05$ *versus* single dose group. Veh: vehicle.

time: F $(4,108)$ = 105.6, $P < 0.0001$, treatment: F $(1,27) = 18.53$, $P = 0.0002$, interaction: F $(4,108) = 3.892$, $P = 0.0054$; multiple dose: time: F $(4,104) = 99.73$, $P < 0.0001$, treatment: F $(1,26)$ = 38.85, $P < 0.0001$, interaction: F $(4,104)$ = 11.66, $P < 0.0001$]. Moreover, edaravone treatment also ameliorated motor dysfunction of MCAO rats on days 1, 3, 5 and 7 [time: F $(4,84)$ = 74.32, $P < 0.0001$, treatment: F $(1,21)$ = 22.31, $P = 0.0001$, interaction: F $(4,84)$ = 5.950, $P = 0.0003$]. Comparing with that of the single dose group, a significant recovery of motor function was observed in the multiple doses group (Fig. 2B). At the 7th day after MCAO surgery, the latency to fall off from rotarod tended to meet that of the sham group. In consistent to the alleviative effect of CPX on MCAO-induced motor functional impairment, post-surgery administration of CPX (3 mg/kg, multiple doses) also significantly reduced the brain infarction volume at 7 days after MCAO surgery (Fig. 2C and D). Moreover, the final survival rates of CPX administration at single dose and multiple doses administration were 75% and 74%, respectively, which were higher than that of vehicle-treated MCAO group (56%), however, there are no statistical significances between different groups (Supporting Information Fig. S4 and Table S3).

3.3. CPX alleviated neuronal loss and neuronal apoptosis in MCAO rats

To clarify whether CPX treatment protected the neurons against ischemic injury, immunofluorescence and western blotting were conducted. In the MCAO alone group, a significant loss of neurons was observed in the ipsilateral cortex as shown by the reduced number of NeuN$^+$ cells and decreased level of NeuN compared to that of the sham group. Administration of CPX significantly reversed the MCAO-induced loss of neurons (Fig. 3A and B and Supporting Information Fig. S5). Similarly, TUNEL-positive cells were found in the ipsilateral cortex of vehicle-treated MCAO rats, which was seldomly observed in the sham group. In contrast, treatment with CPX significantly reduced the percentage of TUNEL-positive cells compared to that of the vehicle-treated MCAO group (Fig. 3C and D).

3.4. CPX inhibited inflammatory responses in MCAO rats

The effects of CPX on the glial activation and inflammatory cytokines were measured in the ischemic brain. First, we found obvious enhancement in the number of IBA-1 and GFAP positive
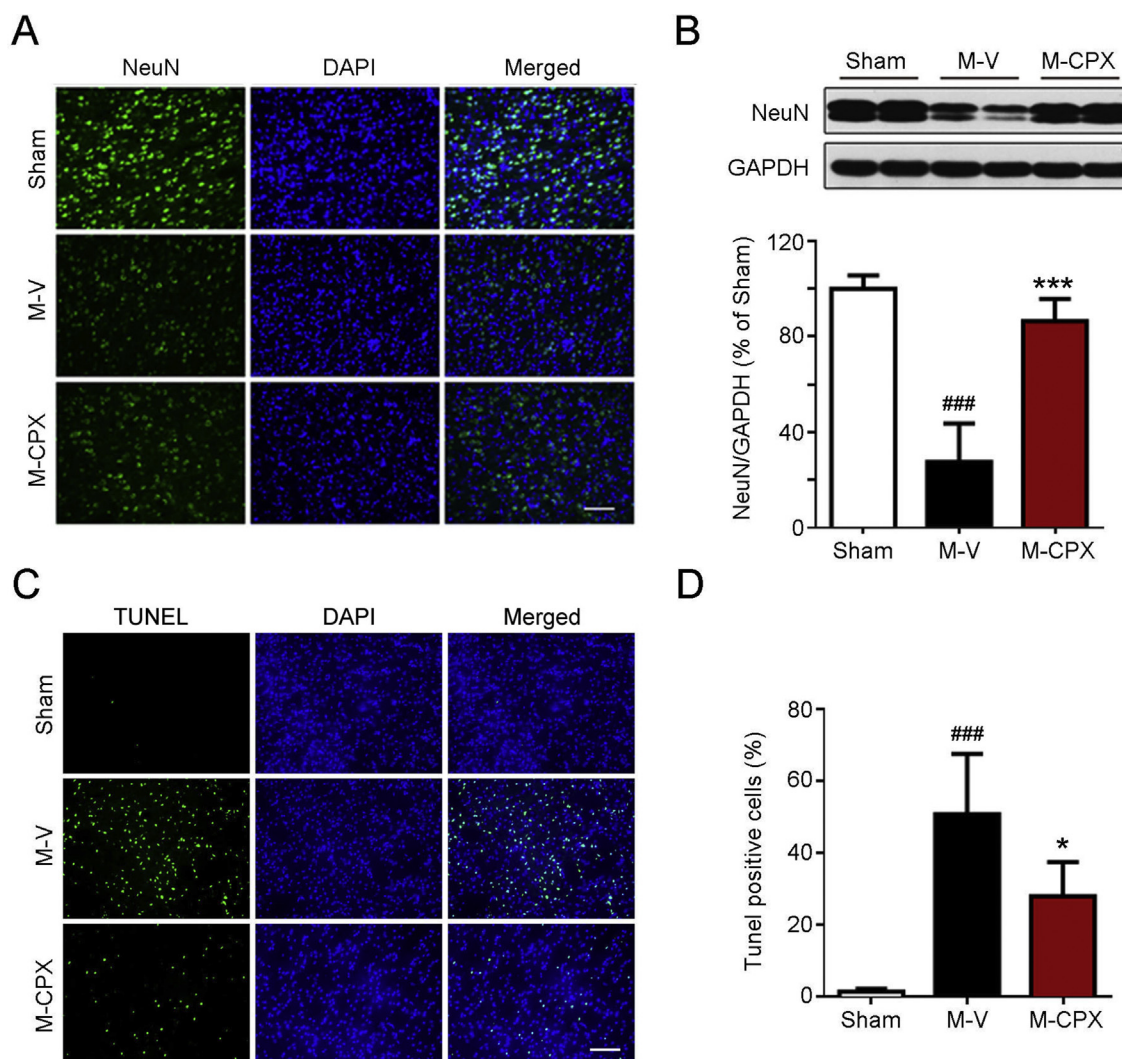
Figure 3 CPX treatment decreased the loss of neurons and apoptosis of neuronal cells in the ipsilateral cortex of MCAO rats. (A) Representative immunostaining for the NeuN in the ipsilateral cortex, scale bar = 100 μm. (B) Western blot for the expression of NeuN, $n = 5$. (C) Representative images of TUNEL staining. Scale bar = 100 μm. (D) Quantitative analysis of TUNEL-positive cells, $n = 5-6$. [###]$P < 0.001$ *versus* sham group, [*]$P < 0.05$, [***]$P < 0.001$ *versus* vehicle-treated MCAO group. M-V: MCAO rats treated with vehicle; M-CPX: MCAO rats treated with 3 mg/kg CPX.

cells in the ipsilateral cortex of the MCAO rats, suggesting significant glial activations. In contrast, the aberrant change on GFAP positive cells was significantly suppressed by CPX treatment, similarly, CPX treatment had a trend to reduce the number of IBA-1 positive cells ($P = 0.06$ *vs.* vehicle-treated MCAO group) (Fig. 4A, B, and Supporting Information Fig. S6). In consistent with the alternations of glial cells, ischemic injury led to a great increase of the TNF-α, IL-1β and IL-6 levels in the ipsilateral cortex of the MCAO rats, whereas the CPX treatment markedly decreased the levels of TNF-α, IL-1β and IL-6 (Fig. 4C). Furthermore, MCAO-induced overexpression of the inflammatory mediator COX-2 was also significantly suppressed by treatment with CPX (Fig. 4C).

3.5. CPX ameliorated BBB damage in MCAO rats

The effect of CPX on BBB permeability after ischemic injury was further determined by Evans blue assay. We observed a marked increase in Evans blue staining in the ipsilateral brain of MCAO rats. However, CPX treatment significantly reduced the amount of Evans blue extravasation in the brain of MCAO rats (Fig. 5A and B). Furthermore, we also assessed the alterations of tight junction proteins after ischemic injury by immunofluorescence and western blotting. Double immunofluorescence results showed that the intensities of CD31 (endothelial marker) and ZO-1 were decreased after ischemic injury, while CPX treatment alleviated the downregulated intensity (Fig. 5C). Similarly, the level of occludin in the MCAO rats was also decreased after ischemic injury, and CPX treatment significantly alleviated the loss of occludin protein (Fig. 5D).

3.6. CPX robustly regulated protein phosphorylation in the OGD-exposed SH-SY5Y cells

As our preliminary results suggested that CPX had a very quick and robust neuroprotective effect against OGD insults, we
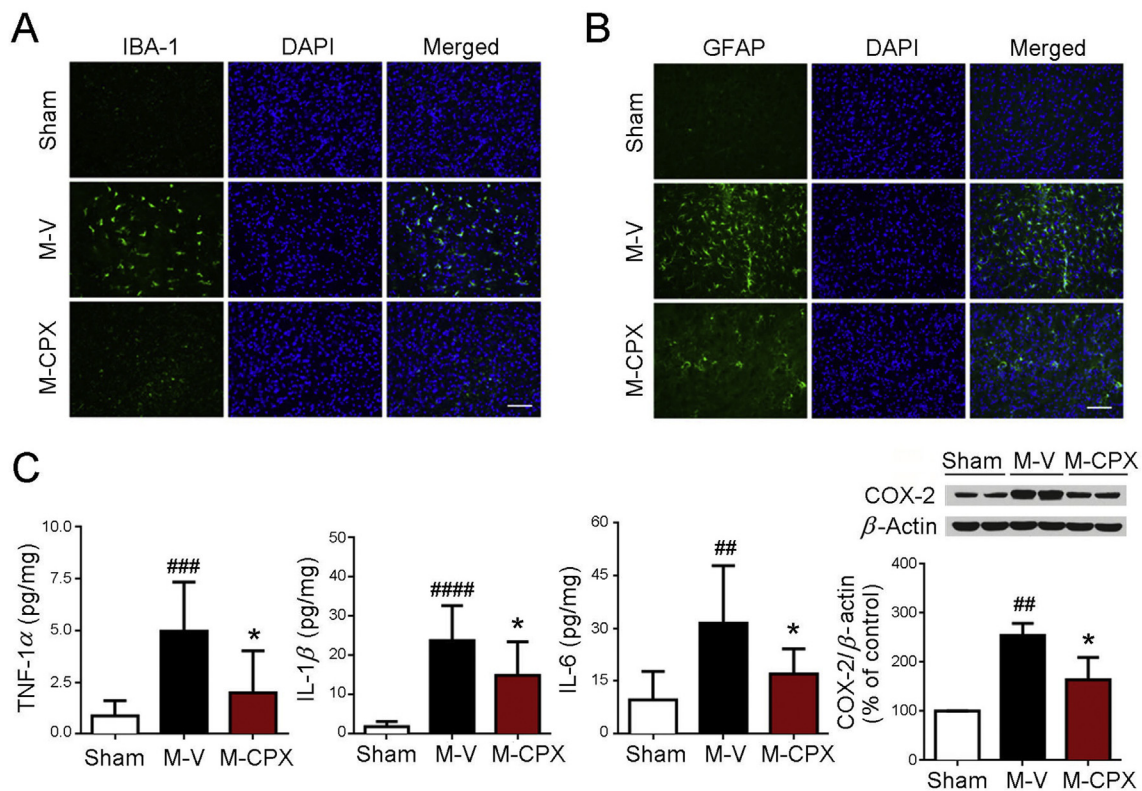
Figure 4 Glial cells activation and inflammatory cytokines production were reduced in the CPX treated MCAO rats. Immunostaining for the IBA-1 (A) and GFAP (B) in the ipsilateral cortex, scale bar $= 100$ μm. (C) The levels of TNF-1α, IL-6, IL-1β ($n = 7-10$), and COX-2 ($n = 4$) in the ipsilateral cortex measured by ELISA or Western blotting. $^{##}P < 0.01$, $^{###}P < 0.001$, $^{####}P < 0.0001$ *versus* sham group, $^{*}P < 0\ 0.05$ *versus* vehicle-treated MCAO group. M-V: MCAO rats treated with vehicle; M-CPX: MCAO rats treated with 3 mg/kg CPX.

therefore utilized mass spectrometry (MS)-based phosphoproteomic approach to study the potential molecular mechanism of CPX in SH-SY5Y cells. A multiplexed sample labeling method TMT10plex followed by Ti^{4+}-IMAC-based phosphopeptides enrichment was employed to quantitatively analyze the phosphorylation changes in "OGD" and "OGD+CPX" compared to "CON" (Supporting Information Fig. S7). Totally, 10,459 phosphosites were identified, of which 7036 were highly reliable phosphosites (site localization probability >0.75) with quantification values. By comparing "OGD+CPX" to "OGD", 130 phosphosites (including 84 up-regulated and 46 down-regulated) in 122 proteins were determined to be significantly regulated by CPX (Fig. 6A). By kinase-substrate prediction analysis of the up-regulated phosphosites, multiple serine/threonine kinases, including cyclin dependent kinase 1/2 (CDK1/2), creatine kinase 1 (CK1), mitogen-activated protein kinase 3 (MAPK3) and PKBα (AKT), seem to be involved in CPX regulation (Fig. 6B). To further investigate the key signaling pathways affected by CPX, we performed the GO biological process enrichment analysis using the regulated phosphoproteins. Cell cycle and chromosome organization are among the top affected processes (Fig. 6C), as also suggested by the potential activation of cell cycle related kinases CDK1/2 (Fig. 6B).

According to above results of phosphoproteomics study and the massive literatures about the critical roles of protein phosphorylation in the pathophysiological of ischemic stroke[26−29], it is suggested that CPX treatment may largely influence the protein serine/threonine kinase activity. Therefore, we further explored the detail protein phosphorylations regulated by serine/threonine

kinases employing the antibody array kit. The intensity of the antibody array (Supporting Information Fig. S8) was summarized as the heat-map (Fig. 6D and Supporting Information Table S4). The phosphorylations of AKT (Ser473), mammalian target of rapamycin (mTOR) (Ser2448), p70S6K (70-kDa ribosomal protein S6 kinase) (Thr389) and GSK-3β (Ser9) were increased after treatment with CPX in the OGD-stimulated SH-SY5Y cells (Fig. 6D, and Table S4). Employing Western blotting analysis, CPX treatment was verified to significantly enhance the level of phosphorylated AKT in the OGD-exposed SH-SY5Y cells (Fig. 6E). Consistent with the changes of AKT, the phosphorylation of GSK-3β, a down-stream kinase of AKT, was also robustly increased after CPX treatment (Fig. 6F). However, the expression of phosphorylated mTOR and its down-stream p70S6K did not change among control, vehicle-treated, and CPX-treated groups in the Western blotting study (Supporting Information Fig. S9). To further determine the relationship between regulation of AKT phosphorylation and protective effect of CPX on neuronal damage, we employed AKT inhibitor, MK2206 in the current study. As shown in Supporting Information Fig. S10, MK2206 at 2 μmol/L significantly suppressed the ameliorative effect of CPX against OGD-induced reduction in cell viability.

3.7 CPX inhibited the cell cycle progression and NO production in LPS-stimulated BV-2 cells

As interfering cell cycle progression was increasing known to play beneficial roles in both neuronal cells and glial cells (reviewed by[30,31]), together with our results from phosphoprotein omics
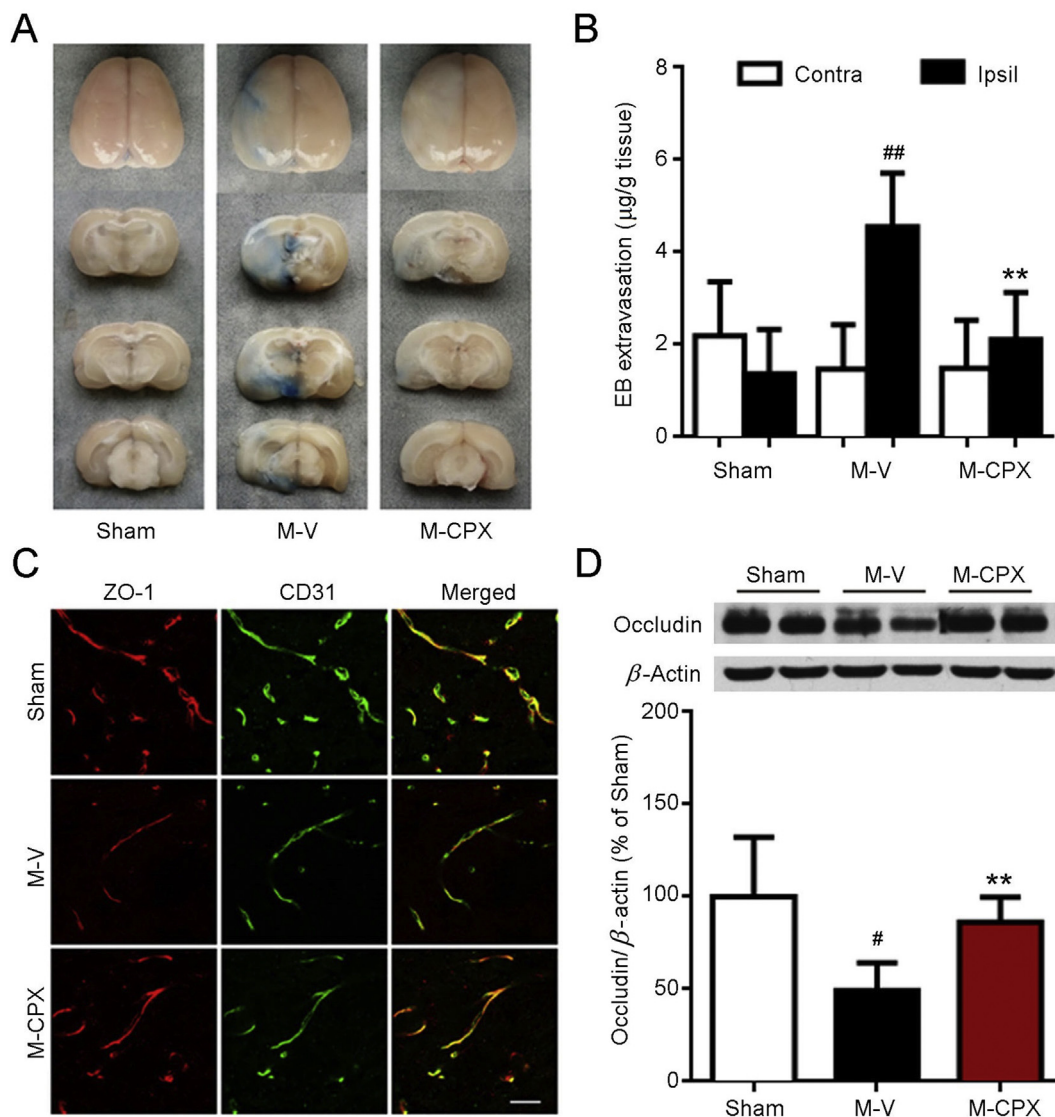
Figure 5 CPX attenuated the BBB disruption and the loss of tight junction protein expression in the brain of rats at 72 h after MCAO. (A) Representative Evans blue extravasation image in the brain of MCAO rats. (B) Quantification of the Evans blue extravasation, $n = 4-7$. (C) Representative image of the double immunofluorescence of CD31 and ZO-1, $n = 4$, scale bar $= 30$ μm. (D) Western-blot of occludin, $n = 4$. [#]$P < 0.05$, [##]$P < 0.01$ *versus* sham group, [**]$P < 0.01$ *versus* vehicle-treated MCAO group. M-V: MCAO rats treated with vehicle; M-CPX: MCAO rats treated with 3 mg/kg CPX.

analysis, cell cycle analysis was conducted in the LPS-stimulated BV-2 microglia by the flow cytometry of PI staining. After CPX treatment, the LPS-stimulated BV-2 cells were enriched with the S phase, but significantly decreased in the G2 phase, compare with that of the LPS group (Fig. 7A and B). Moreover, LPS induced a prominent release of NO in the medium ($P < 0.001$ *versus* control group) of BV-2 cells, which implies the activation of microglia cells, while CPX treatment significantly reduced the LPS-induced overproduction of NO in the BV-2 cells (Fig. 7C).

4. Discussion

Current clinical drugs for the treatment of ischemic stroke are known to inadequately address the underlying complex mechanistic pathogenesis of the disease[9,32]. Here, we systematically verified that anti-fungus drug, CPX, exhibits great potential

against ischemic cerebral injury, using a classical cerebral ischemia model (MCAO rat model). Our results showed that (i) post-ischemic CPX treatment reduced the brain infarction, neurological deficits and brain edema of MCAO rats; (ii) multiple doses post-ischemic administration of CPX further enhanced the long-lasting anti-ischemic effect; (iii) CPX significantly regulated phosphorylation of multiple proteins, especially AKT and GSK3β phosphorylation, under ischemic insult in neuronal cells; (iv) CPX inhibited cell cycle progression and inflammatory response in microglial cells.

In our *in vivo* study, we observed that CPX potently ameliorated cerebral ischemia/reperfusion-induced multi-facet damages in the ischemia brain areas, which may extend its clinical usage upon further investigation. As neuronal death (including apoptosis), glial inflammation, and BBB damage in the ischemic brain area are well-accepted evident pathological changes of brain ischemia[9], the robust effects of CPX against these aberrant
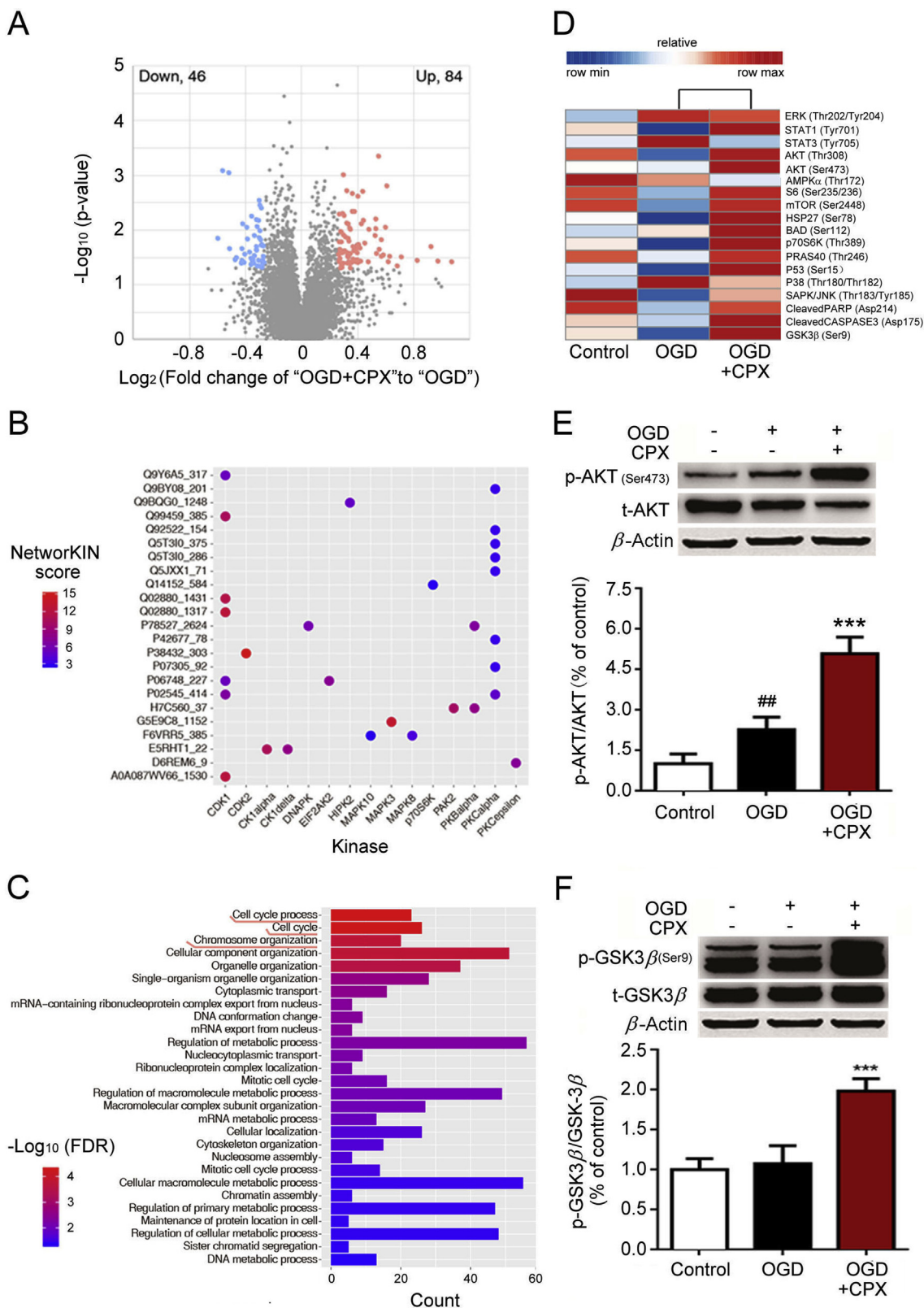
Figure 6 Analysis results from phosphoproteomic study in OGD-exposed SH-SY5Y cells. Cells were collected after OGD exposure followed by another 15 min culture in normal condition. (A) 130 differently regulated phosphosites represented by the volcano plot. It is displayed by $-\log_{10}$ (P-value) versus $\log_2$ of the fold change of "OGD + CPX" to "OGD". Red points: up-regulated sites; blue points: down-regulated sites. (B) The top-scored substrate-kinase prediction result. (C) GO biological process enrichment analysis of changed phosphoproteins. (D) Heat-map of the average RFU intensity of the antibody array. Western blots of phosphorylated AKT (E) and GSK-3β (F) in the OGD-exposed SH-SY5Y cells. $^{\#\#}P < 0.01$ *versus* control group, $^{***}P < 0.001$ *versus* OGD group, $n = 4$.
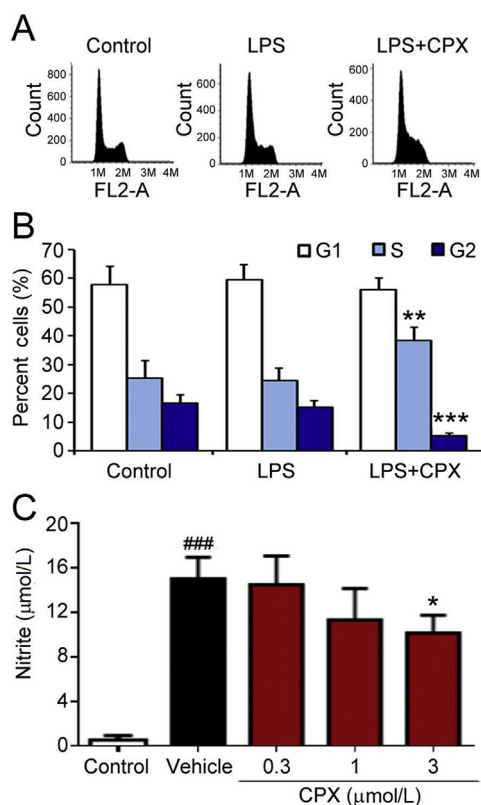
Figure 7 CPX treatment prevented the cell cycle progression and activation of LPS-stimulated BV-2 cells. Representative plots (A) and statistical results (B) of cell cycle analysis by PI staining detected by Flow cytometry. (C) The concentrations of nitrite in the medium after LPS stimulation for 24 h. $^{###}P < 0.001$ versus control group, $^{*}P < 0.05$, $^{**}P < 0.01$, $^{***}P < 0.001$ versus LPS group, $n = 4$.

changes may indicative of the multi-potent capability against ischemic injury. More interestingly, the improved anti-ischemic effect of CPX shown by multiple doses administration further suggest the possible involvement of different pharmacological mechanisms, which also indicates that better efficacy may be achieved through optimization of the drug administration. In order to assess the effect of CPX on MCAO-induced brain injuries without reperfusion, we administered CPX immediately after MCAO surgery, and assessed the changes of infarction volume and neurological function 24 h after MCAO surgery. To a pity, our data revealed that the CPX didn't confer any protection against the MCAO injury without reperfusion (Supporting Information Fig. S11), indicating the distribution of CPX in the ischemic brain area might be necessary for achieving potent anti-ischemic effects as CPX administration without reperfusion may not arrive in the ischemic brain area. Above promising pharmacological effects of CPX administered after reperfusion drive us to further elucidate the molecular mechanisms of CPX.

Recently, "omics" approaches have increasingly recognized to possess great potential to illustrate an exciting new field of target discovery. Among which phosphoprotein omics has received great attention as which enables high-throughput identification of phosphorylation events on metabolic enzymes[33], and it has been well employed to understand the pathophysiological changes of multiple diseases and pharmacological mechanisms of active compounds[34-37]. Our phosphoproteomic results identified 130

significantly regulated phosphosites upon CPX treatment, and the following GO-analysis indicated that many key molecular functions and biological processes were involved. We therefore chose protein serine/threonine kinases and cell cycle phase transition signaling to further study the molecular mechanisms of CPX, as numerous studies have demonstrated that they are both important cascades involved in ischemia/reperfusion[28,30,31,38,39]. Interestingly, we found CPX treatment further enhanced the OGD-induced increase in AKT and GSK3β phosphorylation. Moreover, the neuroprotective effect of CPX against OGD-induced cytotoxicity was markedly weakened after treatment with AKT inhibitor, suggesting that triggering AKT pathway may contribute to the protection of CPX against neuronal damage under ischemic insult. As activation of AKT signaling confer neuroprotection to reduce ischemic damage[38,40,41], together with the evidences that GSK-3β inhibition play beneficial role on improving outcomes after ischemic stroke[42] and agents that potently inhibit GSK-3β activation were found to alleviate the deleterious consequences of stroke[43,44], our finding that targeting AKT-GSK-3β pathway by CPX could effectively contribute, at least partially, to its potent anti-ischemic effects.

Moreover, considerable evidences demonstrated that aberrant cell cycle reactivation exhibited in both glial cells and neurons following ischemia[30,31]. From one aspect, inappropriate cell cycle activation could induce proliferation of astrocyte and microglia and cause inflammatory responses including overproduction of inflammatory cytokines and glial scar formation[30]. From another aspect, delicately control of cell cycle progression is important for neuronal functions as accumulating evidence suggest neuronal cells retain the ability during various neurological injuries including stroke. It is suggested that stroke-stimulated neuronal apoptosis is often associated to the dysregulation of cell cycle[45]. Abnormal phosphorylation of proteins was also found to be involved in the neuronal damage associated with cell cycle activation[46-48]. To our knowledge, we for the first time demonstrated the *in vivo* and *in vitro* effects of CPX on microglial inflammation. We currently observed that CPX effectively regulated the cell cycle progression of LPS-exposed BV-2 cells, which may contribute to the anti-inflammatory effects of CPX in the cellular model. It is interesting that LPS failed to regulate the cell cycle (Fig. 7) and promote the proliferation (Supporting Information Fig. S12) of BV-2 cells, which suggest that the in vivo and in vitro ischemia-associated microglial inflammation are different. Even though, the regulative effect of CPX on cell cycle and cell proliferation may still contribute to its inhibitory effect on inflammatory responses. However, further studies will be necessary to make this conclusion. Similar to the result in the BV-2 cells, we also observed the significant influence of CPX on the cell cycle progression in OGD-exposed SH-SY5Y cells (Supporting Information Fig. S13). Therefore, together with our phosphoproteomic results about the largely influenced phosphorylation sites associated with mitotic nuclear division and mitotic cell cycle phase transition induced by CPX treatment, the regulative effects of CPX in cell cycle progression in both neuronal and glial cells may contribute to the neuronal damage and microglial inflammation under ischemic insult.

Besides that, other pharmacological mechanisms such as angiogenesis and neurogenesis may also partly interpret the anti-ischemic effect of CPX. First, previous studies have demonstrated that CPX treatment could functionally activate hypoxia-inducible factor 1 and elevate the vascular endothelial growth factor level, which may consequently lead to angiogenesis[18]. Second, it is reported that CPX could increase neurite outgrowth in neuronal cells

in the presence of nerve growth factor[49]. As accumulating evidence have already demonstrated the beneficial roles of angiogenesis and neurogenesis against cerebral ischemic damage[50−52], which might additionally interpret the robust *in vivo* effects of CPX against brain ischemia in rats. Moreover, our findings about the superior long-lasting anti-ischemic effect of multiple doses post-ischemic administration of CPX as compared to single dose post-ischemic administration of CPX may give additional support to the involvement of angiogenesis and neurogenesis.

Despite the uncertainty on the precise mode of action, our *in vivo* and *in vitro* multifactorial anti-ischemic results of CPX together with its previously reported good safety and pharmacokinetic profiles[16,53,54] may shed new light on the discovery of potent clinical drug for the therapy of ischemic stroke. However, further systematic studies will be necessary to further illustrate the full potential of bench to bedside research and translate to clinical usage.

5. Conclusions

In summary, our data systematically demonstrated that post-treatment with the anti-fungal drug ciclopirox olamine protected the rat brain against MCAO-induced injuries including brain infarction, neurological dysfunction, apoptosis, inflammation as well as BBB disruption. Moreover, CPX regulated protein phosphorylation under ischemic insults in neuronal cells, especially AKT and GSK-3β phosphorylation, and directly modulated cell cycle and inflammatory responses of microglial cells, which may contribute to its *in vivo* effects on ischemic neuronal damage and microglial inflammation.

Author contributions

Haiyan Zhang and Hongxuan Feng designed the study. Hongxuan Feng, Lingxue Tao and Lei Wu performed the pharmacological studies in MCAO rats. Hongxuan Feng, Qinyuan Zhao, Yemi Gao and Qi Gong performed the pharmacological assays in SH-SY5Y cells and BV-2 cells. Linghao Hu, Fei Mao, and Xiaokang Li synthesized CPX and CPX-associated chemical probes. Jian Li provided the FDA-approved drug library and instructed the chemical synthesis. Hongwen Zhu performed the phosphoproteomic assay. Hu Zhou instructed the phosphoproteomic analysis. Hongxuan Feng and Haiyan Zhang wrote manuscript with input from all authors.

Conflicts of interest

The authors declared no conflicts of interest.

References

1. Cui LY, Zhu YC, Gao S, Wang JM, Peng B, Ni J, et al. Ninety-day administration of dl-3-*n*-butylphthalide for acute ischemic stroke: a randomized, double-blind trial. *Chin Med J (Engl)* 2013;**126**:3405−10.
2. Xue LX, Zhang T, Zhao YW, Geng Z, Chen JJ, Chen H. Efficacy and safety comparison of DL-3-*n*-butylphthalide and cerebrolysin: effects on neurological and behavioral outcomes in acute ischemic stroke. *Exp Ther Med* 2016;**11**:2015−20.
3. Davignon J. Beneficial cardiovascular pleiotropic effects of statins. *Circulation* 2004;**109**:III39−43.
4. Song J, Zhang W, Wang J, Yang H, Zhou Q, Wang H, et al. Inhibition of FOXO3a/BIM signaling pathway contributes to the protective effect of salvianolic acid A against cerebral ischemia/reperfusion injury. *Acta Pharm Sin B* 2019;**9**:505−15.
5. Wang J, Huang L, Cheng C, Li G, Xie J, Shen M, et al. Design, synthesis and biological evaluation of chalcone analogues with novel dual antioxidant mechanisms as potential anti-ischemic stroke agents. *Acta Pharm Sin B* 2019;**9**:335−50.
6. Peng Y, Xu S, Chen G, Wang L, Feng Y, Wang X. L-3-*n*-Butylphthalide improves cognitive impairment induced by chronic cerebral hypoperfusion in rats. *J Pharmacol Exp Ther* 2007;**321**:902−10.
7. Neuhaus AA, Couch Y, Hadley G, Buchan AM. Neuroprotection in stroke: the importance of collaboration and reproducibility. *Brain* 2017;**140**:2079−92.
8. Tymianski M. Combining neuroprotection with endovascular treatment of acute stroke: is there hope?. *Stroke* 2017;**48**:1700−5.
9. George PM, Steinberg GK. Novel stroke therapeutics: unraveling stroke pathophysiology and its impact on clinical treatments. *Neuron* 2015;**87**:297−309.
10. Fu Y, Liu Q, Anrather J, Shi FD. Immune interventions in stroke. *Nat Rev Neurol* 2015;**11**:524−35.
11. Swinney DC, Anthony J. How were new medicines discovered?. *Nat Rev Drug Discov* 2011;**10**:507−19.
12. Guo S, Olm-Shipman A, Walters A, Urciuoli WR, Devito S, Nadtochiy SM, et al. A cell-based phenotypic assay to identify cardioprotective agents. *Circ Res* 2012;**110**:948−57.
13. Schubert D, Maher P. An alternative approach to drug discovery for Alzheimer's disease dementia. *Future Med Chem* 2012;**4**:1681−8.
14. Talevi A. Tailored multi-target agents. applications and design considerations. *Curr Pharmaceut Des* 2016;**22**:3164−70.
15. Martire A, Lambertucci C, Pepponi R, Ferrante A, Benati N, Buccioni M, et al. Neuroprotective potential of adenosine A1 receptor partial agonists in experimental models of cerebral ischemia. *J Neurochem* 2019;**149**:211−30.
16. Shen T, Huang S. Repositioning the old fungicide ciclopirox for new medical uses. *Curr Pharmaceut Des* 2016;**22**:4443−50.
17. Tan T, Marin-Garcia J, Damle S, Weiss HR. Hypoxia-inducible factor-1 improves inotropic responses of cardiac myocytes in ageing heart without affecting mitochondrial activity. *Exp Physiol* 2010;**95**:712−22.
18. Linden T, Katschinski DM, Eckhardt K, Scheid A, Pagel H, Wenger RH. The antimycotic ciclopirox olamine induces HIF-1alpha stability, VEGF expression, and angiogenesis. *FASEB J* 2003;**17**:761−3.
19. Buhler K, Plaisance I, Dieterle T, Brink M. The human urocortin 2 gene is regulated by hypoxia: identification of a hypoxia-responsive element in the 3′-flanking region. *Biochem J* 2009;**424**:119−27.
20. Singh S, Goo JI, Noh H, Lee SJ, Kim MW, Park H, et al. Discovery of a novel series of *N*-hydroxypyridone derivatives protecting astrocytes

against hydrogen peroxide-induced toxicity *via* improved mitochondrial functionality. *Bioorg Med Chem* 2017;**25**:1394−405.

21. Ma TC, Langley B, Ko B, Wei N, Gazaryan IG, Zareen N, et al. A screen for inducers of p21(waf1/cip1) identifies HIF prolyl hydroxylase inhibitors as neuroprotective agents with antitumor properties. *Neurobiol Dis* 2013;**49**:13−21.

22. Longa EZ, Weinstein PR, Carlson S, Cummins R. Reversible middle cerebral artery occlusion without craniectomy in rats. *Stroke* 1989;**20**:84−91.

23. Chen J, Sanberg PR, Li Y, Wang L, Lu M, Willing AE, et al. Intravenous administration of human umbilical cord blood reduces behavioral deficits after stroke in rats. *Stroke* 2001;**32**:2682−8.

24. Zhang L, Chen J, Li Y, Zhang ZG, Chopp M. Quantitative measurement of motor and somatosensory impairments after mild (30 min) and severe (2 h) transient middle cerebral artery occlusion in rats. *J Neurol Sci* 2000;**174**:141−6.

25. Horn H, Schoof EM, Kim J, Robin X, Miller ML, Diella F, et al. KinomeXplorer: an integrated platform for kinome biology studies. *Nat Methods* 2014;**11**:603−4.

26. Takagi N. Protein tyrosine phosphorylation in the ischemic brain. *J Pharmacol Sci* 2014;**125**:333−9.

27. Kisoh K, Hayashi H, Arai M, Orita M, Yuan B, Takagi N. Possible involvement of PI3-K/Akt-dependent GSK-3beta signaling in proliferation of neural progenitor cells after hypoxic exposure. *Mol Neurobiol* 2018;**56**:1946−56.

28. Tuo QZ, Liuyang ZY, Lei P, Yan X, Shentu YP, Liang JW, et al. Zinc induces CDK5 activation and neuronal death through CDK5-Tyr15 phosphorylation in ischemic stroke. *Cell Death Dis* 2018;**9**:870.

29. Li S, Hafeez A, Noorulla F, Geng X, Shao G, Ren C, et al. Preconditioning in neuroprotection: from hypoxia to ischemia. *Prog Neurobiol* 2017;**157**:79−91.

30. Wang W, Bu B, Xie M, Zhang M, Yu Z, Tao D. Neural cell cycle dysregulation and central nervous system diseases. *Prog Neurobiol* 2009;**89**:1−17.

31. Rashidian J, Iyirhiaro GO, Park DS. Cell cycle machinery and stroke. *Biochim Biophys Acta* 2007;**1772**:484−93.

32. Moretti A, Ferrari F, Villa RF. Neuroprotection for ischaemic stroke: current status and challenges. *Pharmacol Ther* 2015;**146**:23−34.

33. Chen Y, Wang Y, Nielsen J. Systematic inference of functional phosphorylation events in yeast metabolism. *Bioinformatics* 2017;**33**:1995−2001.

34. Chen WH, van Noort V, Lluch-Senar M, Hennrich ML, Wodke JA, Yus E, et al. Integration of multi-omics data of a genome-reduced bacterium: prevalence of post-transcriptional regulation and its correlation with protein abundances. *Nucleic Acids Res* 2016;**44**:1192−202.

35. Jaros JA, Martins-de-Souza D, Rahmoune H, Rothermundt M, Leweke FM, Guest PC, et al. Protein phosphorylation patterns in serum from schizophrenia patients and healthy controls. *J Proteomics* 2012;**76**:43−55.

36. Oliveira JM, da Cruz ESCB, Muller T, Martins TS, Cova M, da Cruz ESOAB, et al. Toward neuroproteomics in biological psychiatry: a systems approach unravels okadaic acid-induced alterations in the neuronal phosphoproteome. *OMICS* 2017;**21**:550−63.

37. Solanki HS, Advani J, Khan AA, Radhakrishnan A, Sahasrabuddhe NA, Pinto SM, et al. Chronic cigarette smoke mediated global changes in lung mucoepidermoid cells: a phosphoproteomic analysis. *OMICS* 2017;**21**:474−87.

38. Kilic U, Caglayan AB, Beker MC, Gunal MY, Caglayan B, Yalcin E, et al. Particular phosphorylation of PI3K/Akt on Thr308 *via* PDK-1 and PTEN mediates melatonin's neuroprotective activity after focal cerebral ischemia in mice. *Redox Biol* 2017;**12**:657−65.

39. Mushtaq G, Greig NH, Anwar F, Al-Abbasi FA, Zamzami MA, Al-Talhi HA, et al. Neuroprotective mechanisms mediated by CDK5 inhibition. *Curr Pharmaceut Des* 2016;**22**:527−34.

40. Feng Y, Lu S, Wang J, Kumar P, Zhang L, Bhatt AJ. Dexamethasone-induced neuroprotection in hypoxic-ischemic brain injury in newborn rats is partly mediated *via* Akt activation. *Brain Res* 2014;**1589**:68−77.

41. Li X, Zhang J, Chai S, Wang X. Progesterone alleviates hypoxic-ischemic brain injury *via* the Akt/GSK-3beta signaling pathway. *Exp Ther Med* 2014;**8**:1241−6.

42. Cohen P, Goedert M. GSK3 inhibitors: development and therapeutic potential. *Nat Rev Drug Discov* 2004;**3**:479−87.

43. Collino M, Aragno M, Castiglia S, Tomasinelli C, Thiemermann C, Boccuzzi G, et al. Insulin reduces cerebral ischemia/reperfusion injury in the hippocampus of diabetic rats: a role for glycogen synthase kinase-3beta. *Diabetes* 2009;**58**:235−42.

44. Kelly S, Zhao H, Hua Sun G, Cheng D, Qiao Y, Luo J, et al. Glycogen synthase kinase 3beta inhibitor Chir025 reduces neuronal death resulting from oxygen-glucose deprivation, glutamate excitotoxicity, and cerebral ischemia. *Exp Neurol* 2004;**188**:378−86.

45. Osuga H, Osuga S, Wang F, Fetni R, Hogan MJ, Slack RS, et al. Cyclin-dependent kinases as a therapeutic target for stroke. *Proc Natl Acad Sci U S A* 2000;**97**:10254−9.

46. Aubrecht TG, Faden AI, Sabirzhanov B, Glaser EP, Roelofs BA, Polster BM, et al. Comparing effects of CDK inhibition and E2F1/2 ablation on neuronal cell death pathways *in vitro* and after traumatic brain injury. *Cell Death Dis* 2018;**9**:1121.

47. Iyirhiaro GO, Im DS, Boonying W, Callaghan SM, During MJ, Slack RS, et al. Cdc25A is a critical mediator of ischemic neuronal death *in vitro* and *in vivo*. *J Neurosci* 2017;**37**:6729−40.

48. Jang SW, Liu X, Fu H, Rees H, Yepes M, Levey A, et al. Interaction of Akt-phosphorylated SRPK2 with 14-3-3 mediates cell cycle and cell death in neurons. *J Biol Chem* 2009;**284**:24512−25.

49. Parker EM, Monopoli A, Ongini E, Lozza G, Babij CM. Rapamycin, but not FK506 and GPI-1046, increases neurite outgrowth in PC12 cells by inhibiting cell cycle progression. *Neuropharmacology* 2000;**39**:1913−9.

50. Li Y, Zhang X, Cui L, Chen R, Zhang Y, Zhang C, et al. Salvianolic acids enhance cerebral angiogenesis and neurological recovery by activating JAK2/STAT3 signaling pathway after ischemic stroke in mice. *J Neurochem* 2017;**143**:87−99.

51. Ritzel RM, Patel AR, Spychala M, Verma R, Crapser J, Koellhoffer EC, et al. Multiparity improves outcomes after cerebral ischemia in female mice despite features of increased metabovascular risk. *Proc Natl Acad Sci U S A* 2017;**114**:E5673−82.

52. Chen CK, Hsu PY, Wang TM, Miao ZF, Lin RT, Juo SH. TRPV4 activation contributes functional recovery from ischemic stroke *via* angiogenesis and neurogenesis. *Mol Neurobiol* 2018;**55**:4127−35.

53. Lukasova I, Muselik J, Vetchy D, Gajdziok J, Gajdosova M, Jurica J, et al. Pharmacokinetics of ciclopirox olamine after buccal administration in rabbits. *Curr Drug Deliv* 2017;**14**:99−108.

54. Coppi G, Silingardi S. HPLC method for pharmacokinetic studies on ciclopirox olamine in rabbits after intravenous and intravaginal administrations. *Farmaco* 1992;**47**:779−86.